ARPGE: a computer program to automatically reconstruct the parent grains from electron backscatter diffraction data

Cyril Cayron

CEA-Grenoble, DRT/LITEN, 17 rue des Martyrs, 38054 Grenoble, France. Correspondence e-mail: cyril.cayron@cea.fr

A computer program called *ARPGE* written in Python uses the theoretical results generated by the computer program *GenOVa* to automatically reconstruct the parent grains from electron backscatter diffraction data obtained on phase transition materials with or without residual parent phase. The misorientations between daughter grains are identified with operators, the daughter grains are identified with indexed variants, the orientations of the parent grains are determined, and some statistics on the variants and operators are established. Some examples with martensitic transformations in iron and titanium alloys were treated. Variant selection phenomena were revealed.

1. Introduction

The mechanical properties of many materials, such as steels and titanium alloys, rely on a fine microstructure constituted of lath-shaped micro- or nanometric interconnected daughter grains generated by a phase transformation. Very often the transformation is complete and there is no retained parent phase, or only a very small content. However, knowledge of the parent grains is important in metallurgy. Let us consider one example. During the elaboration of martensitic steels, the impurities migrate at high temperature into the austenitic grains boundaries and, after the martensitic transformation, they form brittle intermetallic particles that are deleterious to the toughness (Cahn *et al.*, 1992). Moreover, since the prior austenitic grain boundaries are often depleted in chromium, they are also more sensitive to corrosion. Consequently, the size of the prior austenitic grains is a key microstructural parameter in the mechanical models of martensitic steels. Knowledge of possible variant selection is also important in metallurgy and this phenomenon must be controlled in order to optimize the texture by thermo-mechanical treatments. For instance, in shape memory alloys, the mechanical properties come from variant selection during deformation or heating treatment (see, for example, Kaouache *et al.*, 2006). Generally speaking, there is an important need in the metallurgical community to have a computer program that automatically reconstructs the parent grains and establishes statistics on the variant selection.

Electron backscatter diffraction (EBSD) is a technique used in scanning electron microscopy that allows phase identification and orientation mapping with an angular resolution of ∼1° and a spatial resolution of ∼10 nm. We have recently developed a method based on a general crystallographic theory (Cayron, 2006) to automatically reconstruct the parent grains from EBSD data of materials constituted only of daughter grains (Cayron *et al.*, 2006). The aim of the present paper is to present a computer program called *ARPGE*, for automatic reconstruction of parent grains from EBSD data, which uses this method and integrates new functionalities. It reconstructs the parent grains, determines their orientation and texture, identifies the variants, and establishes some statistics that can help to under-

stand the variant selection mechanisms. The software treats any structural phase transformation materials.

2. Description of the program

ARPGE has been written in Python, which is a multi-platform, interpreted and object-oriented language (Martelli, 2006; see also http://www.python.org/). The main menu of *ARPGE*, presented in Fig. 1, is constructed using the graphical user interface library TkInter. The program needs the following.

(i) The phase transformation data, *i.e.* the parent and daughter point groups, the orientation relationship, and the resulting theoretical groupoid composition table generated by the computer program *GenOVa* (Cayron, 2007). These data can be imported or created from the 'Phase Transition' menu.

(ii) The experimental EBSD map acquired with commercial EBSD equipment such as *HKL* or *TSL* and imported in the 'Files' menu.

The 'Filters' menu allows removal of 'spikes' (indexation errors) and dilation of the pixels to remove badly indexed areas. The 'Daughter Identification' menu allows us to identify the daughter grains according to a criterion on the misorientation angle ('Tolerance for Grain Identification') and to a criterion on the minimum number of pixels per grain ('Minimum Accepted Grain size'). This reconstruction is performed in two steps, firstly by comparing only the Euler angles (leading to pre-grains) and secondly by checking if the misorientations between the pre-grains are close to a symmetry operation. This part of the program is not optimized and the calculations are quite long in comparison with commercial software. The new and optimized part is the 'Parent Reconstruction' menu. The program checks if the misorientations between neighboring daughter grains are close to the theoretical operators and, if the result is positive, it checks if the composition of these operators is in agreement with the theoretical groupoid composition table. This parent grain reconstruction is performed in two steps: a nucleation step with a low tolerance angle (usually 3–5°) and a growth step with a larger tolerance angle (usually 10–15°). These two angular parameters, 'Tolerance for Parent Grain Nucleation' and 'Tolerance for Parent
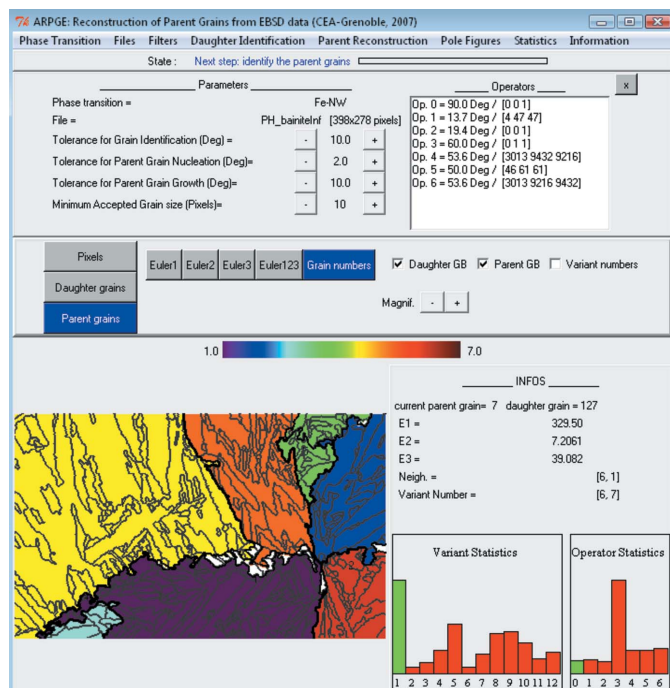
 1183

Figure 1
Main menu of the *ARPGE* program with, for example, some austenitic grains reconstructed in a bainitic steel.

Grain Growth', are the only parameters needed for the reconstruction. The details are reported by Cayron *et al.* (2006), but now the 'tolerated misindexation' parameter is not needed. The reconstruction is saved automatically and, if it is not complete, the user can continue the process by increasing the two tolerance angles. In general, one or two cycles are enough to reconstruct more than 80% of the map. The calculations are quite fast because they rely on comparison of integers and there is no need to solve any equation. For example, on a 1.5 GHz computer with 500 Mb RAM, it takes 10 min for a steel constituted of 100 martensitic grains reconstructed into six austenitic grains, and 1 h for a similar steel containing 1000 martensitic grains reconstructed into 100 austenitic grains.

In addition to the work of Cayron *et al.* (2006), *ARPGE* now integrates new possibilities. The variant indices are automatically calculated and can be seen in the map. These indices are integers between 1 and the number of variants. The number 1 is attributed to the largest daughter grain encountered during the nucleation step. The orientations of the parent grains are automatically determined and can be visualized with the 'Pole Figures' menu on stereographic or equal-area pole figures simply by double-clicking on the parent grains in the map. Special misorientations between the parent grains, such as $\Sigma 3$ twins, can be determined. The global pole figure corresponding to the texture of the parent grains can also be drawn. In the 'Statistics' menu, the indices of variants and operators are represented on charts that allow us to see at first glance a possible variant selection phenomenon. The reconstructed parent data can be exported to files compatible with commercial computer programs.
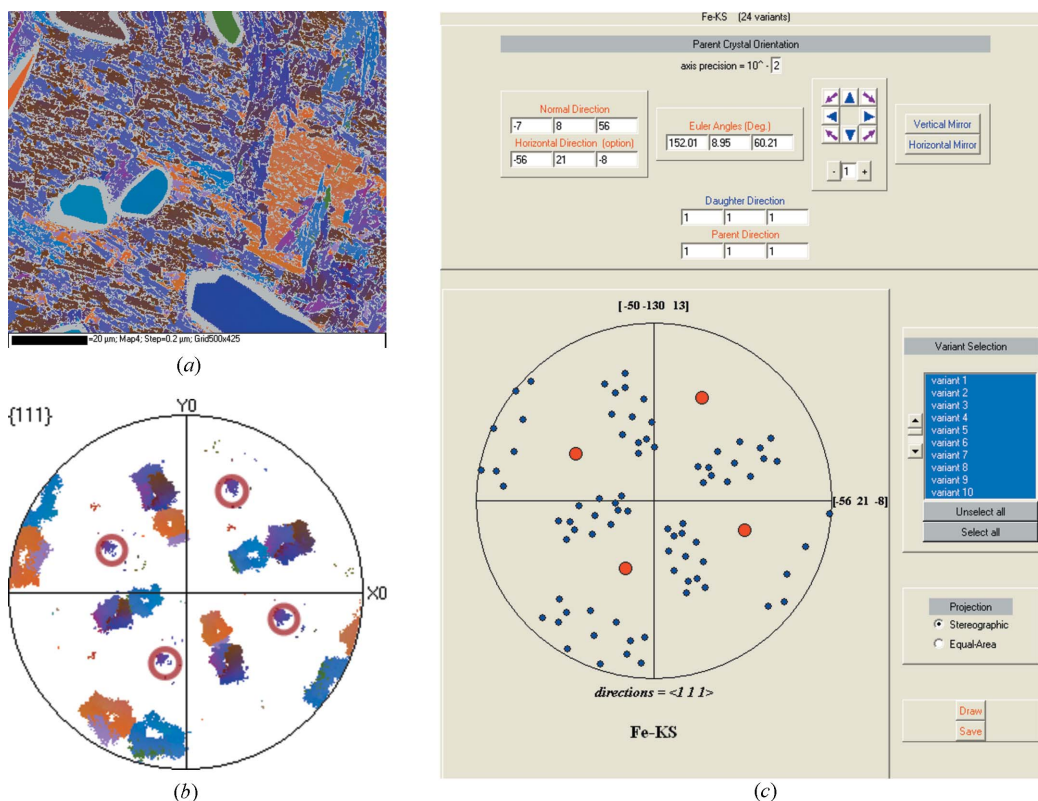

Figure 2
A martensitic iron (courtesy of J. Michael). (*a*) EBSD orientation map of the martensitic grains and (*b*) corresponding pole figure. *ARPGE* finds only one austenitic grain, whose orientation is indicated by the red circles superimposed on the pole figure. (*c*) According to that orientation, theoretical pole figure of the 24 variants (blue spots) in a Kurdjumov–Sachs orientation relationship with the parent crystal (red spots).
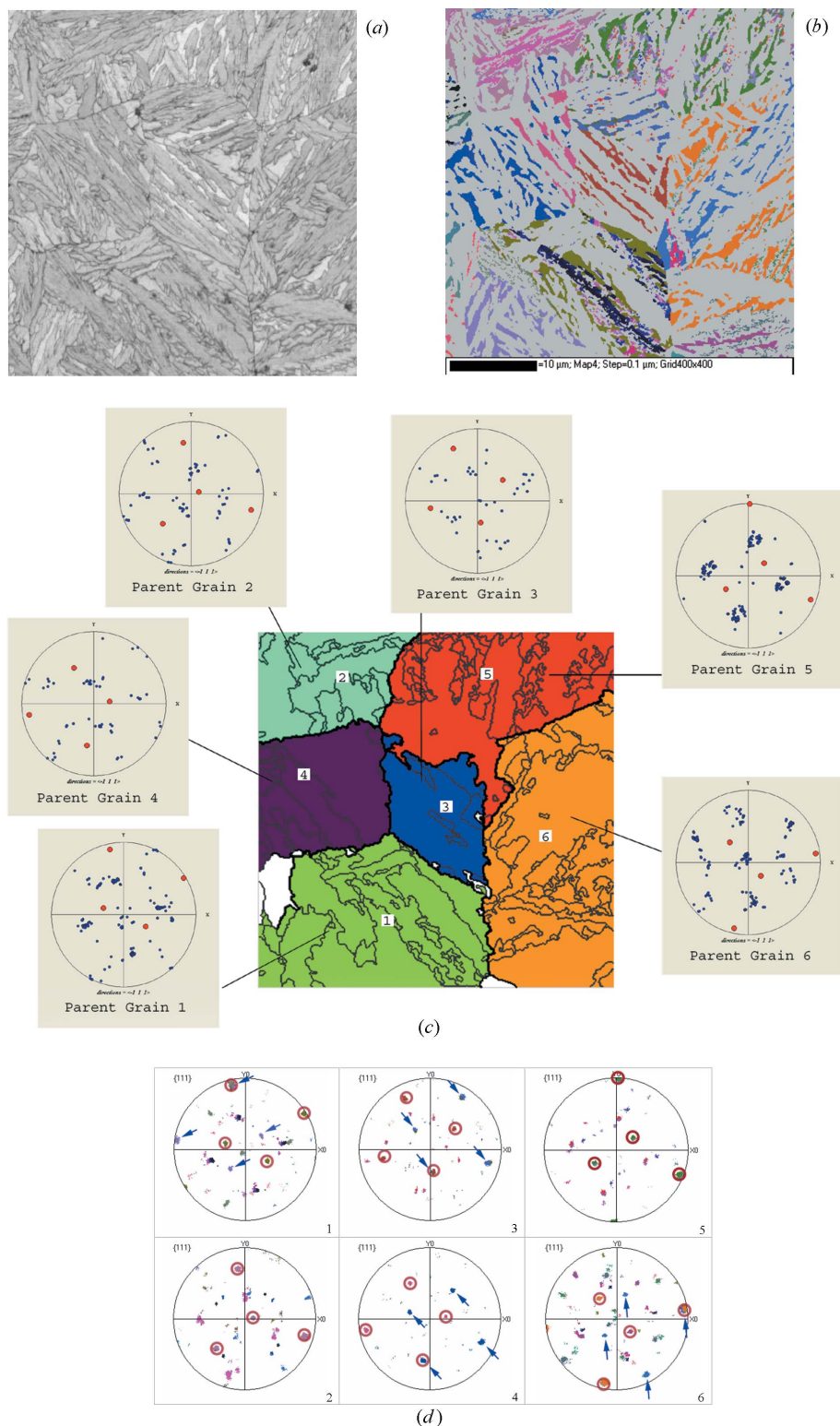
(a)

(b)

Parent Grain 2

Parent Grain 3

Parent Grain 5

Parent Grain 4

Parent Grain 1

Parent Grain 6

(c)

(d)

3. Some examples

3.1. Bainitic/martensitic irons and steels

The first example is a martensitic iron from a meteorite (courtesy of J. Michael, Sandia National Laboratories, USA). The EBSD map has been acquired by detecting only the martensitic phase, *i.e.* the body-centered cubic (b.c.c.) structure. The austenitic phase, *i.e.* the face-centered cubic (f.c.c.) structure, was not considered at all. The orientations of the different martensitic grains are coded by colors representing the Euler angles and illustrated in the orientation map of Fig. 2(a) and in the associated pole figure (Fig. 2b). *ARPGE* finds only one austenitic grain, whose orientation is indicated by the red circles superimposed on the pole figure (Fig. 2b). One can check that this calculated orientation is the correct one by comparing the experimental pole figure (Fig. 2b) of the martensitic grains with the theoretical pole figure simulated with the *GenOVa* program and reported in Fig. 2(c). One may also notice that the red circles corresponding to the calculated austenite orientation coincide with some experimental directions attributed to the martensite phase. The martensitic directions are not present in the theoretical simulation of Fig. 2(c). This is a result of a misindexation between the austenite and the martensite phases during the EBSD acquisition.[1] Therefore, the coincidence between the reconstructed red circles and these experimental directions can be considered as another proof for the efficiency of the reconstruction.

The second example is a bainitic steel (courtesy of P. H. Jouneau, INSA-Lyon, France). Since the proportion of residual austenite is more important in that material, both bainite (b.c.c.) and austenite (f.c.c.) phases have been taken into consideration during the EBSD acquisition. The quality map is presented in Fig. 3(a). The orientation of the retained austenite is given in Fig. 3(b). We then tested *ARPGE* to check if it could effectively find the austenitic grains and their orientations only from the bainitic data. Only the experimental bainitic orientations were loaded into the *ARPGE* program. Assuming a bainitic transformation with a Nishiyama–Wasserman (NW) orientation relationship, *ARPGE* finds six

Figure 3
Bainitic steel (courtesy of P. H. Jouneau). (a) Quality index map. (b) Orientation map of the austenite phase. (c) *ARPGE* finds six austenitic grains (only the information on the bainitic phase has been taken into account in the reconstruction). The experimental orientations of the bainitic grains inside the reconstructed austenitic grains and the calculated orientations of the austenitic grains are represented by the ⟨111⟩ directions in the pole figures by blue and red spots, respectively. (d) The experimental orientations of the residual austenite corresponding to the six reconstructed grains are reported and the calculated orientations are superimposed with red circles. One may check the perfect agreement between the calculated and the experimental orientations of the austenitic grains. The other spots come from twinned austenite (blue arrows) and some bainitic grains misindexed as austenite.

---

[1] The algorithms for the determination of the crystal orientation by EBSD take mainly into account the angles between the crystallographic planes, and the difference of the lattice parameters is only of secondary order. The problem of misindexing between the martensite and austenite phases can be minimized by increasing the number of bands during the acquisition.

austenitic grains, represented in Fig. 3(c). Their orientations are given by the red spots in the pole figures. The experimental orientations of the retained austenite corresponding to these reconstructed areas are reported in Fig. 3(d). In that figure, we have also superimposed the calculated austenitic orientations of Fig. 3(c) by using red circles. All the experimental austenitic orientations are located inside the calculated red circles. This proves the efficiency and the high precision of the reconstruction algorithms used in *ARPGE*. Nevertheless, some other orientations have not been detected [blue arrows in Fig. 3(d) and other small dots]. These orientations correspond to twins of the austenitic grains 1, 3, 4 and 6 and also to bainite wrongly indexed as austenite (see footnote 1). By a careful examination of the data, we have concluded that the twins could not have been found because they have generated only 'common' variants. Let us explain. We have proved in §9.2 of Cayron (2006) that, assuming an NW orientation relationship, four variants are always sufficient to reconstruct without ambiguity the orientation of the austenitic

crystal, and we have shown that an austenitic crystal can share three common bainitic variants with its Σ3 twin. These common variants are those encountered in the case of Fig. 3. We believe that the presence of only these common variants in the twinned austenite is not a coincidence but results from stress accommodation mechanisms during the bainitic transformation. Such a hypothesis would need deeper study. This example shows the intrinsic limit of our reconstruction program; there is no method based only on orientation measurements that allows the distinction between untwinned and twinned austenite if the twinning process generates only the three common variants.

The third example is a martensitic steel used in nuclear pressured water reactors (courtesy of J. M. Gentzbittel, CEA-Grenoble, France). There is absolutely no residual austenite. The EBSD orientation map of the martensite is given in Fig. 4(a); the reconstructed austenite is presented in Fig. 4(b). More than 100 austenitic grains could be identified and their orientation determined. Some
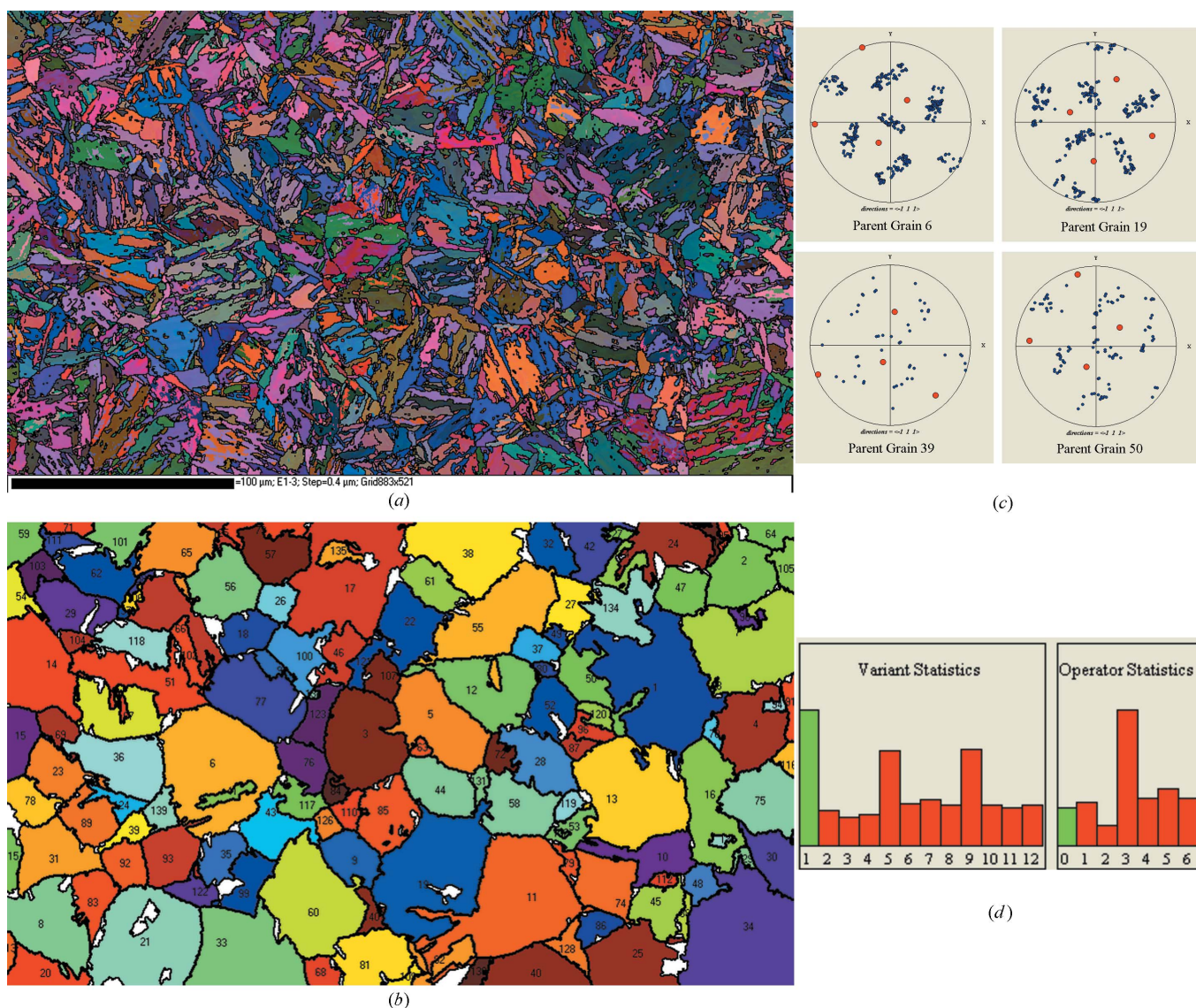

Figure 4
Martensitic steel (courtesy of J. M. Gentzbittel). (a) Orientation map of the martensite. (b) Reconstructed austenite (the boundaries of the martensitic grains are not shown here for better visibility). (c) Pole figures of some of the reconstructed austenitic grains with their calculated orientations (red spots) and with the experimental orientations of the martensitic grains (blue spots). (d) Statistical bar charts on the distributions of the variant indices and operator indices (the percentages of encountered variants or operators are given as a function of their indices).

examples of the pole figures of the reconstructed austenitic grains are presented in Fig. 4(c). The reconstruction works even for small austenitic grains containing few martensitic grains (see grain 39 for example). The number of austenitic grains is enough to establish some statistics on the variant and operator indices, as illustrated in Fig. 4(d). The variant α_1 is the most frequent because the programs

always choose the index 1 for the larger grain during the nucleation process. In future versions of *ARPGE* we could attribute a random index between 1 and the theoretical number of variants to suppress this effect. It may be noticed that the most frequent operator is O_3. This is a clear example of a variant selection phenomenon. Actually, this is not a surprise. The operator O_3 corresponds to a rotation of $60°$ around the $[110]_\alpha = [111]_\gamma$ direction (Cayron *et al.*, 2006); it links the three variants that share a common $(111)_\gamma$ plane (these three variants are also the 'common' variants for twinned austenite). The fact that the most frequent variants after the variant α_1 are the variants α_5 and α_9 results from the high frequency of operator 3 (material property), the high frequency of the variant α_1 (algorithm effect) and the fact that operator O_3 contains the arrows α_{15} and α_{19} (theory).

3.2. Titanium alloys

ARPGE has been written to work with any structural phase transition. We have checked, for instance, its performance for the Burgers transition where the parent cubic β phase is transformed into the daughter hexagonal α phase. The first example is a wrought titanium Ti-6Al-4V alloy used in the Vulcain engine of the Ariane 5 rocket. The EBSD orientation map of the α grains is given in Fig. 5(a), and the reconstructed parent β grains are presented in Fig. 5(b). Pole figures of two reconstructed grains are presented in Figs. 5(c) and 5(d). It can be seen that the calculated $\langle 110 \rangle_\beta$ directions coincide with the experimental $\langle 001 \rangle_\alpha$ directions, in agreement with the Burgers orientation relationship. Moreover, the patterns formed by the α grains coincide with the theoretical *GenOVa* simulations (not presented here). The reconstruction took 10 min.

The last example is a Ti-6Al-4V titanium alloy elaborated by powder metallurgy and studied for the future engine Vinci of the Ariane 5 rocket. The EBSD orientation map of the α grains is given in Fig. 6(a), and the reconstructed parent β grains are presented in Fig. 6(b). Despite the presence of small highly deformed and disoriented α grains, the reconstruction seems to be correct. For example, one may check on the pole figure (Fig. 6c) of the largest reconstructed grain that, here again, the calculated $\langle 110 \rangle_\beta$ directions coincide with the experimental $\langle 001 \rangle_\alpha$ directions, in agreement with the Burgers orientation relationship. The reconstruction lasted 30 min. One may also notice in the statistics presented in Fig. 6(d) that the operator O_1 is the most frequent and that operator O_2 is nearly absent. This result is quite surprising. One would have expected to find a high proportion of operator O_2 because this operator corresponds to a rotation of $10.5°$ around the hexagonal c axis, *i.e.* the misorientation between the two variants that share a common $(110)_\beta$ plane (see Table 4 of Cayron, 2006). A global understanding including the shape of the variants and the elastic field in the set of variants could probably explain such a feature.

4. Conclusions and perspectives

ARPGE is a program that reconstructs the parent grains from the data obtained on the EBSD maps of phase transition materials. There is no need for any retained parent phase. The program works for any structural phase transformation. We have checked its validity for martensitic and bainitic transitions in irons and steels and for Burgers transitions in titanium alloys. The first menus ('Files', 'Filters' and 'Daughter Identification') are the same, although less optimized and effective, as those of commercial EBSD software. The other menus are new. The principle of the method relies on checking the coherence of the operator composition (Cayron *et al.*, 2006). The parent grains are reconstructed, their orientation calculated and the
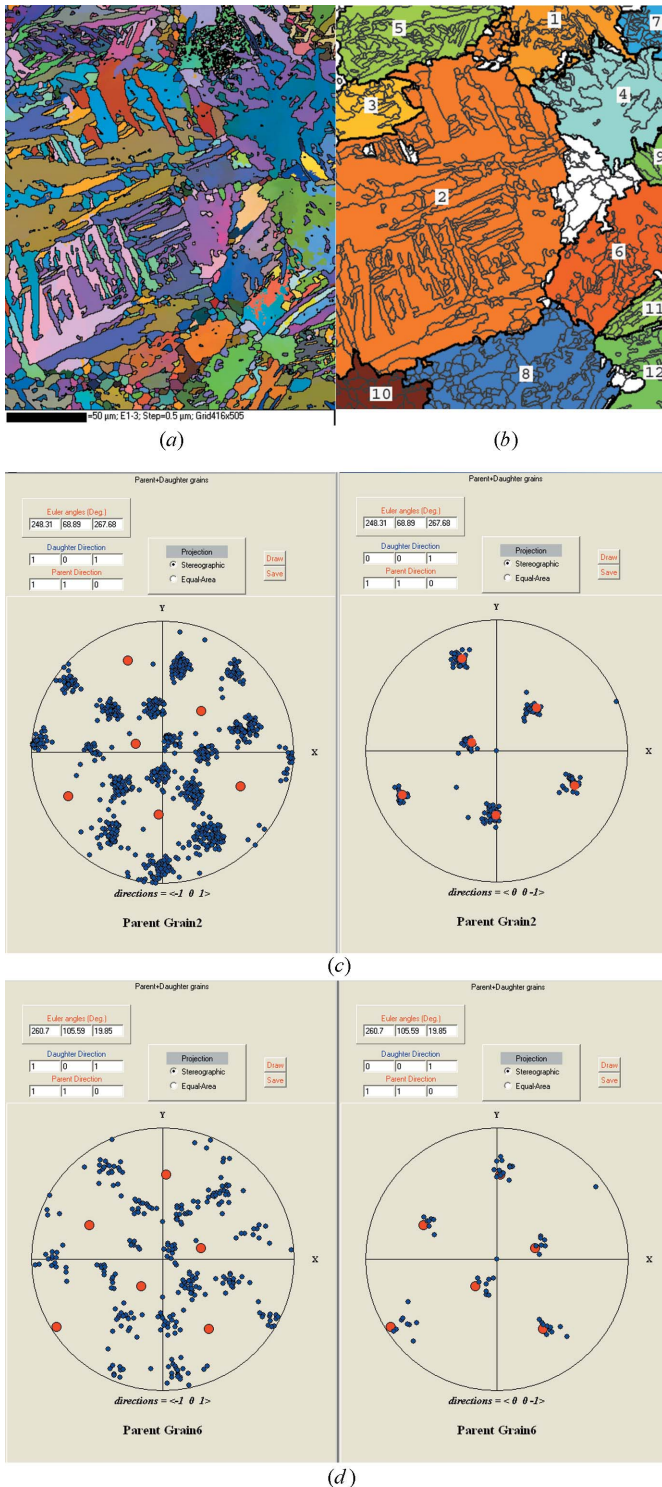

Figure 5
Wrought titanium Ti-6Al-4V alloy. (a) EBSD orientation map of the α grains. (b) Reconstructed parent β grains. Pole figures of (c) grain 2 and (d) grain 6 with the projection of the $\langle 101 \rangle_\alpha$ directions (on the left) and $\langle 001 \rangle_\alpha$ directions (on the right).
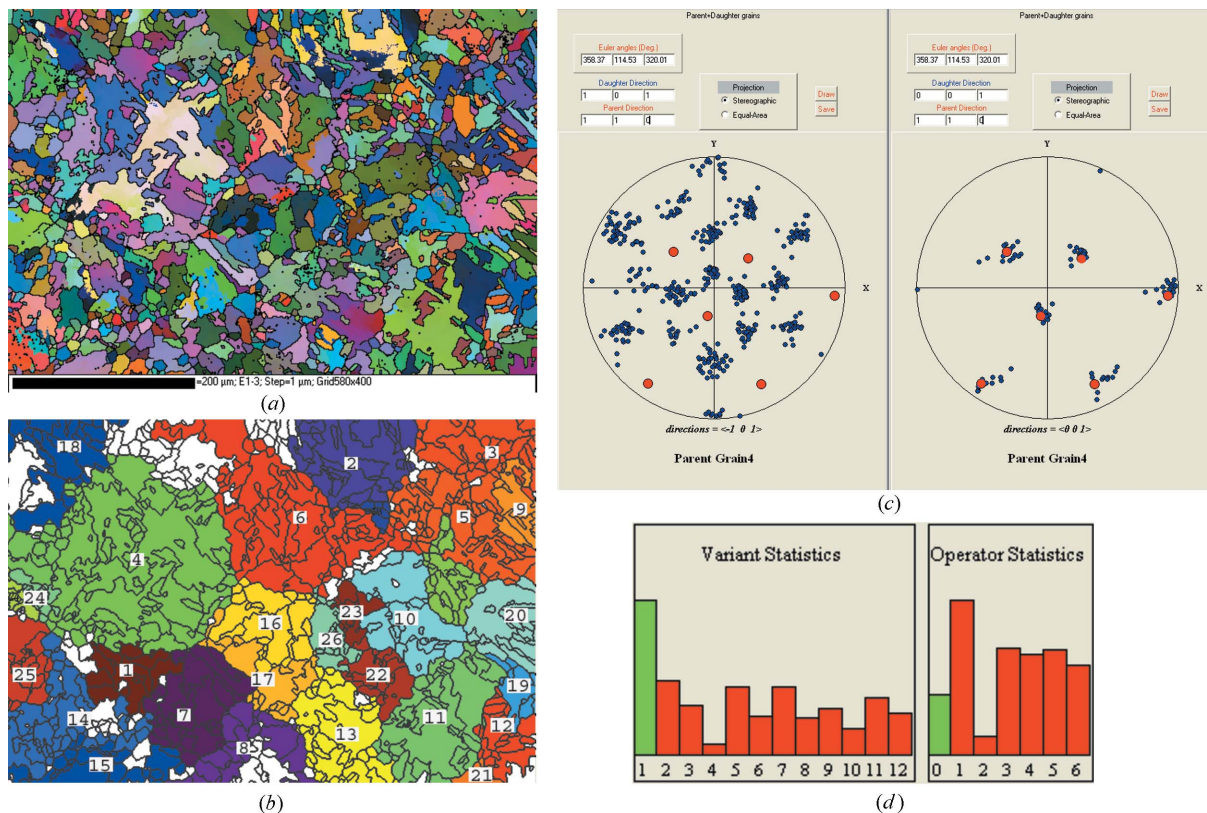
Figure 6
Powder metallurgy Ti-6Al-4V titanium alloy. (*a*) EBSD orientation map of the α grains. (*b*) Reconstructed parent β grains. (*c*) Pole figures of grain 4 with the projection of the $\langle 101 \rangle_\alpha$ and $\langle 001 \rangle_\alpha$ directions. (*d*) Statistical bar charts on the variant and operator indices.

daughter grains are identified with indexed variants. Some statistical charts on the variant and operator indices are established. Variant selection phenomena can be easily visualized on these charts.

References

Cahn, R. W., Haasen, P. & Kramer, E. J. (1992). *Materials Science and Technology, A Comprehensive Treatment*, Vol. 7, *Constitution and Properties of Steels*, pp. 74–76. Weinheim: VCH.

Cayron, C. (2006). *Acta Cryst.* A**62**, 21–40.

Cayron, C. (2007). *J. Appl. Cryst.* **40**, 1179–1182.

Cayron, C., Artaud, B. & Briottet, L. (2006). *Mater. Charact.* **57**, 386–401.

Kaouache, B., Inal, K., Berveiller, S., Eberhardt, A. & Patoor, E. (2006). *Mater. Sci. Eng. A*, **438**, 773–778.

Martelli, A. (2006). *Python in a Nutshell*, 2nd ed. Cambridge: O'Reilly.